(15) Naegele, D.; Yoon, D. Y. *Appl. Phys. Lett.* **1978**, *33*, 132.
(16) Douglass, D. C.; McBrierty, V. J.; Wang, T. T. *J. Chem. Phys.* **1982**, *77*, 5826. *Appl. Phys. Lett.* **1982**, *41*, 1051.
(17) Mizuno, T.; Nakamura, K.; Murayama, N.; Okuda, K. *Polym. Prepr. Jpn.* **1981**, *30*, 676.
(18) Cessac, G. L.; Curro, J. G. *J. Polym. Sci., Polym. Phys. Ed.* **1974**, *12*, 695.
(19) Tashiro, K.; Kobayashi, M.; Tadokoro, H. *Polym. Bull. (Berlin)* **1978**, *1*, 61.
(20) Nye, J. F. "Physical Properties of Crystals"; Oxford University Press: Oxford, 1957.
(21) Tashiro, K.; Kobayashi, M., unpublished data.
(22) Tashiro, K.; Takano, K.; Kobayashi, M.; Chatani, Y.; Tadokoro, H. *Ferroelectrics* **1984**, *57*, 297.
(23) Yagi, T.; Higashihata, Y.; Fukuyama, K.; Sako, J. *Ferroelectrics* **1984**, *57*, 327.

Fluorescence Anisotropy Decay Studies of Local Polymer Dynamics in the Melt. 2. Labeled Model Compounds of Variable Chain Length

Jean Louis Viovy,* Curtis W. Frank,† and Lucien Monnerie

Laboratoire de Physico-Chimie Structurale et Macromoleculaire (L.A. CNRS 278), ESPCI, 75231 Paris Cedex 05, France. *Received March 15, 1985*

ABSTRACT: The fluorescence anisotropy decay (FAD) of a series of 9,10-dialkylanthracenes, with alkyl substituents ranging from 6 to 16 CH_2 groups, embedded in a melt of unlabeled polybutadiene is investigated in the temperature range 210–350 K. The results are compared with different theoretical dynamic models relevant for flexible alkyl chains or for polymers by using the quantitative evaluation procedure applied to labeled polybutadiene in the previous paper of this series. The orientation autocorrelation function (OACF) presents a nonexponential character that increases progressively with the length of the alkyl tail. For tails with 14 carbon atoms and more, the OACF corresponds very accurately to the 1-D diffusion observed in long-chain labeled polymers. This result probes rather unambiguously the chain length necessary for the "polymer-like" 1-D diffusion behavior to settle. Also, the evolution of the correlation times with the temperature and with the size of the molecule supports the idea, developed recently by Helfand and co-workers, that this 1-D diffusion corresponds to correlated conformational jumps.

I. Introduction

In the previous paper of this series, we presented fluorescence anisotropy decay (FAD) experiments performed at LURE-ACO, Orsay, France. Using synchrotron radiation as an exciting source, we recorded the orientation autocorrelation function (OACF) of a labeled polybutadiene chain embedded in a matrix of similar unlabeled polybutadiene in the time window 0.1–70 ns and in the temperature range 223–353 K. The experimental results have been compared with various models for main-chain polymer motions proposed in the literature.[2-7]

The shape of the OACF, which remains almost homothetic when the temperature is varied, is very similar to the one observed in dilute solutions.[7] Recent single-chain models of the dynamics, such as the Hall–Helfand[6] or generalized diffusion and loss[7] models, fit the data correctly at the present experimental precision. From these observations, we concluded that the major origin of the nonexponential character of the single-bond OACF is the connectivity of the chain. In comparison with dynamics in dilute solution, the surrounding chains affect segmental motions by means of an increase in the friction coefficient, but they do not seem to modify seriously their specific dynamic behavior.

We also observed that the orientation relaxation of the label follows the same temperature law as macroscopic properties (i.e., WLF equation[8,9]). Such a result implies that the local chain motions observed by FAD in polybutadiene are involved in the glass transition phenomenon. If one considers the experimental time scale (0.1–70 ns), the size of the label, and the amplitude of orientation relaxation required to affect the OACF, it is reasonable to assume that these chain motions correspond to conformation changes. However, it would be interesting to investigate their scale more quantitatively.

In the present paper, we present synchrotron-excited FAD experiments performed on a series of flexible fluorescent probes (9,10-dialkylanthracene) embedded in a matrix of nonfluorescent polybutadiene. By studying the evolution of the OACF as a function of the length of the alkyl tail, we aimed at further information about the molecular origin of the observed orientation relaxation. For instance, if, as we suspected, the nonexponential character of the OACF is mainly due to chain connectivity, it should increase with substituent length, and the rate of this increase should give direct information on the scale of the motions involved. We were also interested in the coupling between the flexible probes and the polymer matrix and in a comparison between the behavior of the probe and that of labeled long-chain polybutadiene.

In section II, the preparation of the samples and the experimental technique are briefly reviewed (for a more complete description please refer to part 1 of the series).[1] The experimental correlation functions and some general results are presented in section III. In sections IV and V, we compare quantitatively these results with relevant theoretical models, namely the Jones and Stockmayer[4] model, which considers flexible chains starting from the "short molecule" side, and the Hall and Helfand[6] and generalized diffusion and loss[7] models, which start from an "infinite chain" representation. Temperature effects are discussed in section VI, and the general molecular conclusions which can be drawn from the present study are summarized in section VII.

† Permanent address: Department of Chemical Engineering, Stanford University, Stanford, CA 94305.

0024-9297/85/2218-2606$01.50/0

Table I
Mean Correlation Time Analysis of the Fluorescence Anisotropy Decays of the C_n Probes

C_6		C_8		C_{10}		C_{14}		C_{16}	
T, K	$\bar{\tau}$, ns	T, K	$\bar{\tau}$, ns	T, K	$\bar{\tau}$, ns	T, K	$\bar{\tau}$, ns	T, K	$\bar{\tau}$, ns
264.9	49.0	265.2	60.4	213.9		269.7	47.7	215.2	
281.0	16.6	294.4	11.1	250.4	139	282.4	28.1	238.3	266
301.5	5.2	302.5	7.0	267.2	56.1	291.3	19.6	260.5	70.3
321.9	2.2	322.1	2.7	282.3	28.5	302.8	13	277.0	23.3
		342.7	1.36	294.5	13.4	314.6	8.0	292.0	17.7
				302.8	10.0	329.2	5.21	308.5	9.83
				309.1	7.1	355.1	2.93	323.0	5.82
				319.9	4.1				
				342.7	1.6				

Table II
Best-Fit Parameters Using Different Models for the Different C_n Probes at Similar Temperatures

n (T, K)	model	χ^2	r_0	τ_1, ns	τ_2, ns	A_1	A_2	τ_2/τ_1
6 (301.5)	1E, J_0	1.51	0.284	5.17				
	J_2	4.55	0.341	4.47				
	J_4	6.60	0.402	2.60				
	J_6	28.6	0.465	1.77				
	2E	1.04	0.300	0.98	5.57	0.037	0.263	
	GDL	1.16	0.291	6.14	9.3			1.5
8 (302.5)	1E, J_0	4.34	0.273	7.00				
	J_2	4.37	0.321	6.18				
	J_4	22.0	0.359	4.14				
	J_6	37.9	0.354	4.15				
	2E	1.04	0.307	0.92	7.9	0.063	0.244	
	GDL	1.85	0.288	5.84	13.48			2.3
10 (302.6)	1E, J_0	7.68	0.265	8.87				
	J_2	2.47	0.305	8.21				
	J_4	11.8	0.326	6.29				
	J_6	17.8	0.319	6.56				
	2E	1.12	0.312	1.07	10.8	0.085	0.277	
	GDL	2.43	0.288	4.43	22.6			5.1
10 (302.8)	1E, J_0	3.84	0.268	9.99				
	J_2	2.51	0.283	10.7				
	J_4	7.01	0.289	9.45				
	J_6	8.65	0.286	9.68				
	2E	1.19	0.300	1.81	12.8	0.080	0.220	
	GDL	1.27	0.263	6.75	21.6			3.2
14 (302.8)	1E, J_0	8.31	0.270	13.0				
	J_2	1.47	0.282	14.7				
	J_4	1.46	0.289	13.2				
	J_6	1.65	0.290	13.0				
	2E	1.22	0.311	3.07	27.0	0.143	0.168	
	GDL	1.32	0.280	4.13	78.5			19
16 (308.5)	1E, J_0	17.5	0.261	9.83				
	J_2	4.24	0.300	9.36				
	J_4	2.49	0.325	7.17				
	J_6	3.53	0.312	6.87				
	2E	2.18	0.310	1.97	18.5	0.145	0.167	
	GDL	2.10	0.297	2.14	67			31

II. Experimental Section

The linear 9,10-dialkylanthracenes used in the present study were synthesized in our laboratory following an original method.[10] They correspond to the formula

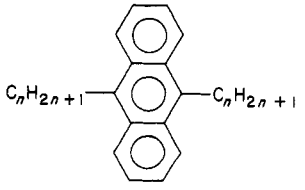

with n an even number ranging from 6 to 16. In the following, we abbreviate these compounds as "C_n".

The polymer matrix was the same non-cross-linked polybutadiene (PB) as used in the previous study,[1] provided by the Michelin Co. Chloroform solutions containing the polymer and the probe were prepared, and the solvent was removed by a progressive procedure, ended in vacuum. Concentrations were adjusted to maintain an optical density less than 0.08 in the final sample, in order to avoid any energy transfer. Previous studies have shown that for probes as short as the ones studied here, the dispersion in PB is random and no segregation occurs.[11] The preparation of cells has been described in part I. The FAD experiments were performed on the Cyclosynchrotron LURE-ACO, Université Paris-Sud and CNRS, Orsay, France. The source and the fluorescence device have been described previously.[12]

III. Results

The OACF of the C_n probes with n less than 6 behaves in a rather complicated manner when n is varied. Indeed, for these probes we expect that the friction of the alkyl tails is smaller than that of the anthracene fluorescent group so that the dynamics are those of a mainly rigid object (see the discussion in section IV). On the contrary, a rather monotonic evolution is observed for n equal to or greater than 6. Thus, we performed the present study on probes in this last class, namely n = 6, 8, 10, 14, and 16. We expect them to be the most interesting to investigate the dynamics of flexible linear chains, since the influence

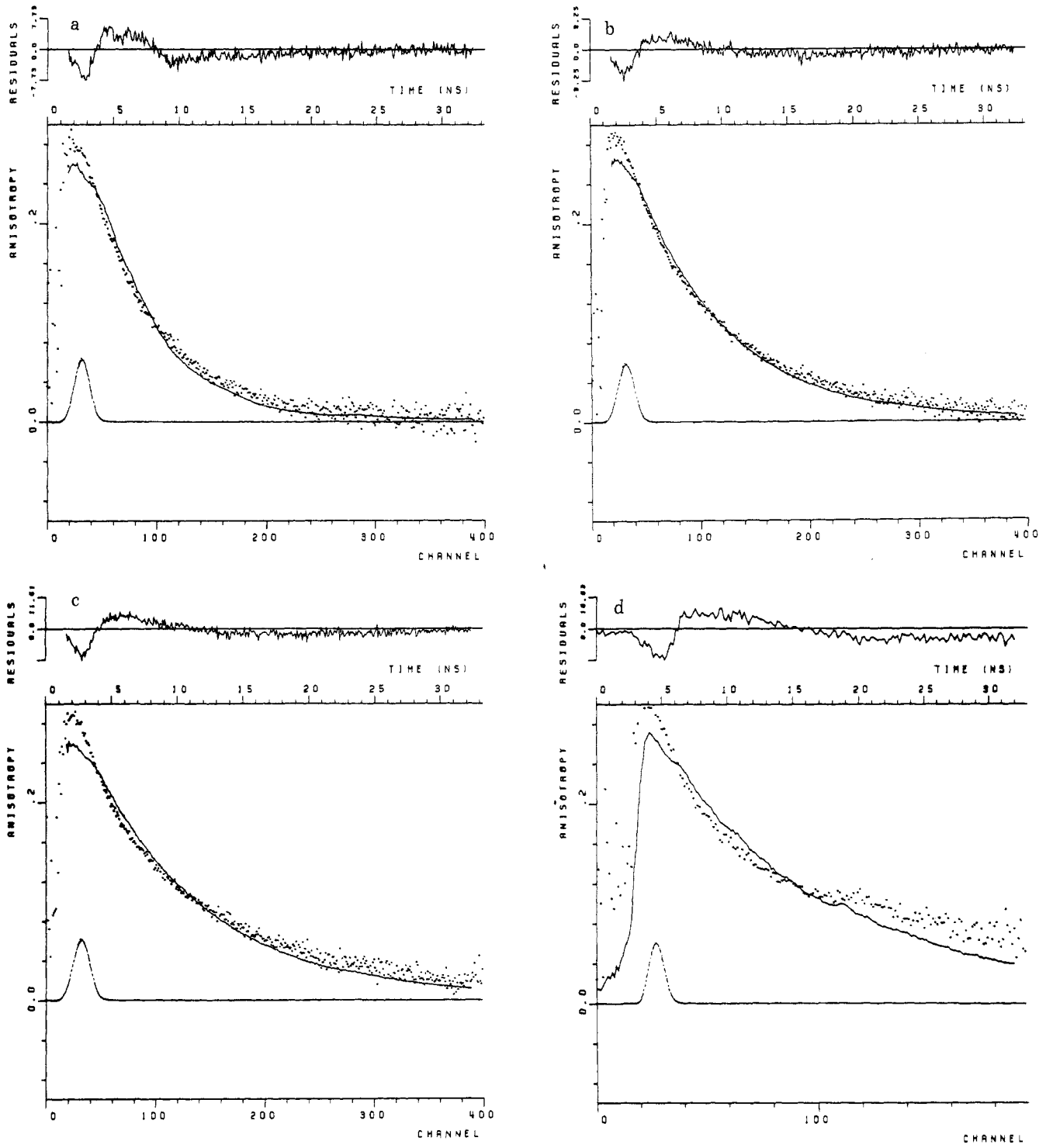

Figure 1. Experimental fluorescence anisotropy decay (dots) and best-fit 1-exponential reconvolution (continuous line) for different C_n probes at similar temperatures: n = 6 (1a), 8 (1b), 10 (1c), 14 (1d).

of the rigid fluorescent group must be smaller. In the case of C_{10}, two series of experiments were performed with a time interval of more than 1 year on samples prepared independently.

These two series are presented separately in all the following to give an idea of the reproducibility of experiments, which is about 10% for the interesting parameters (see, for instance, Tables I and II).

The experimental fluorescence anisotropy decay curves for the various probes at approximately similar temperatures are presented in Figure 1. As explained in paper I, the FAD corresponds to the OACF of the transition moment of the probe, convoluted by the profile of the excitation pulse. In the present set of experiments, this pulse is generally short as regards the observed phenomena, and the main qualitative features of the OACF's can be visualized directly on the experimental FAD's. However, all the quantitative results presented in the following were obtained by using an iterative reconvolution fitting procedure, which accounts for the shape of the pulse and for the random error in the experimental data. (For more details, see paper 1).

Visual observation of the OACF's shows that the orientation decorrelation rate decreases when the size of the alkyl substituents is increased. During the time of the experiment, the anisotropy decreases to zero in the case of C_6, but it remains significantly higher than zero for C_{16}. This is confirmed by a crude 1-exponential best-fit iterative

reconvolution procedure: the mean correlation time increases with n, although there is a modest scatter in the results (see Table I).

The shape of the OACF also varies with the length of the tails, as shown by a visual comparison to the best-fit 1-exponential reconvoluted anisotropy (full lines): the longer the alkyl tail, the more pronounced is the nonexponential character. Of course, fitting a 2-exponential expression leads to a much better fit (compare, for instance, the 2-exponential best fit obtained for C_{14}, Figure 2a, and the corresponding 1-exponential best fit, Figure 2b). Quantitative results are given in Table II.

The way to interpret these results deserves some comment. In principle, χ^2 is the main indication of the quality of a fit. For purely statistical errors, χ^2 should be equal to 1, and any systematic deviation increases the measured value. However, the systematic deviations are not due only to the model used in deconvolution. The experiment also involves a small part of nonrandom errors, such as small fluctuations in the pulse shape, nonrandom noise, finite precision of polarization calibration, etc. Thus, for a given actual experiment, even a "perfect model" may not reach $\chi^2 = 1$. The actual practical minimum of χ^2 generally depends on the set of data and on such parameters as the period of the synchrotron cycle at which the experiment is performed and so on. Thus, we never compare the values of χ^2 obtained for different experiments, but only the values obtained when different models are fitted to the same data set. In that case, the amount of nonrandom error is the same, and small discrepancies in χ^2 are significant. As discussed in part 1, other information can be used to differentiate models, such as the reasonable physical range for the best-fit parameter r_0 (about 0.20–0.32 for anthracene) or the variation of the best-fit parameters upon changes in the fitting window.

In the present case, the χ^2 values obtained with two exponentials are good, but the physical meaning of such a fit is questionable: the theoretical treatment for rotational diffusion of an anisotropic rigid rotor with the transition moment parallel to one of the principal axes leads to a biexponential OACF, with some conditions on the parameters.[13] These conditions are not always fulfilled by the best-fit 2-exponential parameters obtained for the C_n probes in the present study. Apart from this difficulty, it is obvious that our probes are not rigid at all, and a physically reasonable model should account for this flexibility.

Indeed, the alkyl substituents are similar to very short polyethylene chains, and it seemed interesting to discover if their motions could be described by models dedicated to polymer dynamics, already used in the previous study on long polybutadiene chains.[1] Thus, we applied our fitting procedure to the data by using the Jones and Stockmayer,[4] Hall and Helfand,[6] and generalized diffusion and loss[7] models. In the following, we use the 2-exponential fit as a mere phenomenological curve-fitting expression: Our experience[1,7,14,15] indicates that such a four-parameter expression is versatile enough to fit rather well any experimental anisotropy and reach values of χ^2 very close to the "ideal" ones (i.e., the ones that should be obtained with a theoretical model reflecting ideally the actual dynamic behavior of the probe).

IV. Comparison to the Jones and Stockmayer Model

In the Jones and Stockmayer (JS) model, a finite chain with an odd (and generally moderate) number of bonds performs "3-bonds" motions on a tetrahedral lattice. The OACF of the central bond of the chain is then a sum of exponentials depending on the number of bonds taken into account. This arbitrary truncation of the chain was used by the authors as a simplified way to account for the damping of orientational memory along a long polymer chain. However, it should depict even better the actual situation investigated here, i.e., the OACF of the central bond of a finite flexible alkyl chain. The simplifications that remain in the model as regards the actual C_n probes are the following: (i) The bonds of the probe certainly do not follow accurately a tetrahedral lattice. (ii) The conformation of the alkyl tails is not equally weighted, as in the model. (iii) The anthracene group probably modifies the dynamics.

For these reasons, we do not expect that the "bond" in the model corresponds to an actual bond in the probe. To be more general, we consider this theoretical "bond" as an "equivalent kinetic unit"; we are not trying to associate it a priori with a given sequence in the actual probe.

All the experimental FAD's were tentatively fitted to the expressions derived by Jones and Stockmayer for chains with 0, 2, 4, and 6 equivalent units on each side of the investigated bond (hereafter abbreviated as J_u, where u is the number of equivalent units). Following this notation, the total number of equivalent units in a "J_u" probe is $2u + 1$. The corresponding expressions are listed in ref 4. (The J_0 expression is a single exponential, discussed in the previous section.) The quantitative results for different probes at similar temperatures are given in Table II, and the evolution of the fit as a function of the number of equivalent units for the same dataset (here C_{14} at 302.8 K) is presented in Figure 2, parts b and e. Most often, when u is increased, χ^2 decreases then increases, without reaching values comparable with the 2-exponential ones (Table II). Indeed, since the JS expressions can be derived only for even integer numbers of equivalent units in each tail, there is no reason why the analytical expressions should always correspond to the integer numbers of carbon atoms in our probes.

This difficulty, due to the discrete nature of the model, can be partly overcome by considering the values obtained for $u = 0$, 2, 4, and 6 as sampling points on a continuous $\chi^2 = f(u)$ curve. One also assumes that the correct noninteger value of u should lead to a value of χ^2 close to the 2-exponential "ideal" one. The different curves $\chi^2 = f(u)$ plotted for different probes in Figure 3 are thus interpolated by knowing four sampling points and the ordinate of the minimum. They clearly show that the χ^2 minimum moves toward high u values when the number of carbon atoms in the tail, n, is increased. Approximate values of $u_m(n)$, the abscissa of the minima, are drawn and plotted in Figure 4 as a function of n. For C_6, u_m is very close to 0: the tails are probably too short to control the dynamics of the observed transition moment. For this probe, and shorter ones, the motions are dominated by the friction of the anthracene, and models for flexible chains are probably not relevant. For higher values of n, u_m increases rather linearly with n. The slope indicates that one "equivalent kinetic unit" in the model corresponds approximately to three carbon atoms in aliphatic chains in a PB matrix. The precision for long tails is low because the change in the OACF, and thus the change in χ^2, is very weak for high values of u. Indeed, Jones and Stockmayer have shown that for such relatively high values of u the OACF predicted by their model is very close to the shape derived by using models for an infinite flexible chain.[4] The rather good fit obtained for probes C_{14} and C_{16} and expressions J_4 and J_6, in spite of the limitations of the models, seems to indicate that the 1-dimension diffusion

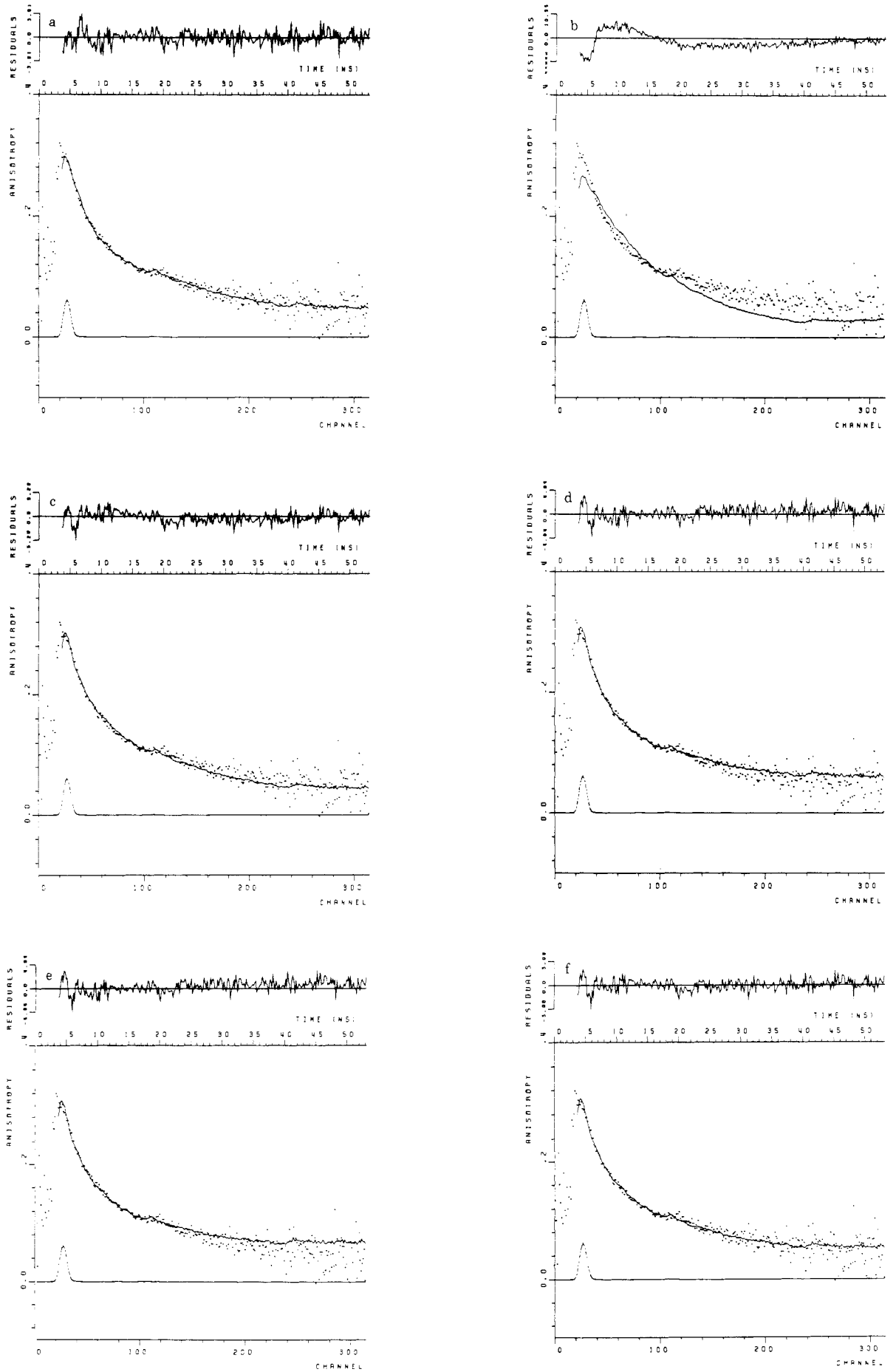

Figure 2. Best-fit reconvolution for probe C_{14} at 29.8 °C using different models: 2-exponential (a), 1-exponential or J_0 (b), J_2 (c), J_4 (d), J_6 (e), and GDL (f). (The weighted residuals are plotted in the upper scale.)

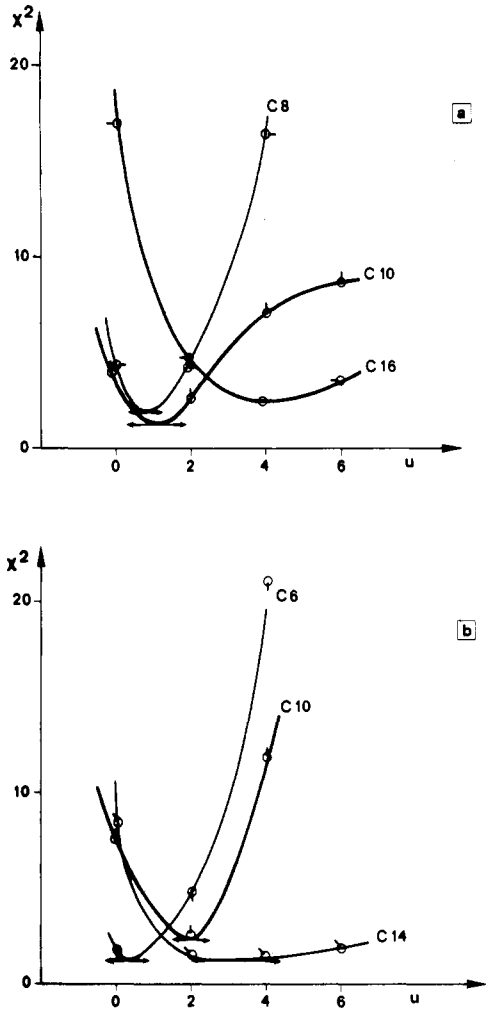

Figure 3. χ^2 as a function of the number of equivalent units for different probes. (For clarity, the results, including two independent series of experiments corresponding to C_{10}, are plotted separately.)

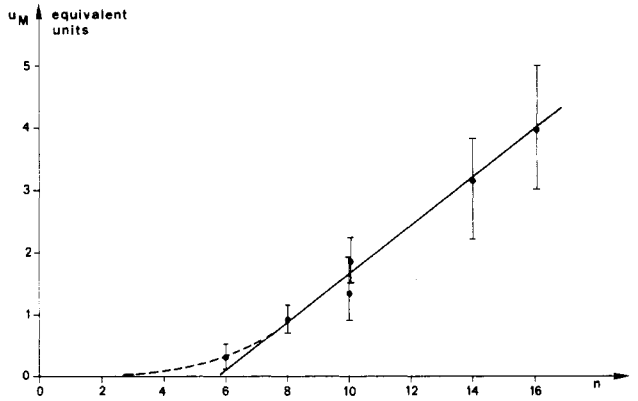

Figure 4. Adjusted number of equivalent units in the JS model as a function of the number of carbon atoms in the alkyl tail of the probe.

of orientation, which characterizes the dynamics of polymers, is efficient even on rather short portions of chain. Similar conclusions have been reached recently in a quasi-elastic neutron-scattering study of short crown polyethers.[16]

Following these observations, it is natural to fit the same data with models proposed for long-chain polymer dynamics and to investigate their limits when they are applied to the C_n probes, considered as very short model molecules for labeled polyethylene.

Table III
Comparison of the Best-Fit Parameters Obtained for Different Probes at Different Temperatures by Using the Hall–Helfand and Generalized Diffusion and Loss Models

n (T, K)	model	χ^2	r_0	τ_1, ns	τ_2, ns	τ_2/τ_1
C_{14}						
269.7	HH	2.35	0.299	44.7		
	GDL	2.17	0.301	19.6		
282.4	HH	3.41	0.299	21.0		
	GDL	2.12	0.304	8.25		
291.3	HH	1.98	0.298	13.0		
	GDL	1.16	0.308	4.83		
302.8	HH	1.42	0.277	8.87	450	51
	GDL	1.32	0.281	4.13	78	19
314.6	HH	1.48	0.272	5.28	55	11
	GDL	1.22	0.282	2.19	32	15
329.2	HH	1.82	0.261	3.47	24	7
	GDL	1.61	0.273	1.35	18	13
355.1	HH	1.24	0.244	2.17	10	5
	GDL	1.10	0.255	0.83	7.8	9
C_{10} 302.8	HH	1.30	0.261	12.6	28	2.2
	GDL	1.27	0.263	6.75	22	3.2
C_{16} 308.5	HH	3.19	0.290	5.29	249	47
	GDL	2.10	0.297	2.14	67	31

V. Comparison to the Diffusion and Loss Models

In part 1, we have shown that two expressions based on modified Bessel functions well accounted for the OACF of labeled polybutadiene: the Hall–Helfand (HH) expression

$$f_{HH}(t) = r_0 \exp(-t/\tau_2) I_0(t/\tau_1) \exp(-t/\tau_1)$$

and the "generalized diffusion and loss" expression

$$f_{GDL}(t) = r_0 \exp(-t/\tau_2)(I_0(t/\tau_1) + I_1(t/\tau_1)) \exp(-t/\tau_1)$$

In both expressions, the t/τ_1 term corresponds to a 1-D diffusion of orientation along the chain sequence, and the t/τ_2 term corresponds to a loss of orientation or, equivalently, to a damping of the diffusion. The I_1 term in the GDL model has been introduced to account for some perturbations due to the label, but the two models contain the same physics and correspond to the same representation of the chain. As in previous studies,[1,7] we observed that the GDL expression generally leads to better results than the HH one (see, for instance, the results for C_{14} given in Table III). The χ^2 values are lower, and the ratio τ_2/τ_1 is defined more precisely. However, one can also check in Table III that the evolution of the best-fit parameters as a function of the temperature or as a function of n is similar. In the following, we base our discussions on the GDL results, but the physical conclusions are the same for the two models.

The evolution of the best-fit parameters as a function of n in the GDL model is given in Table II. For C_6, χ^2 is rather close to the 2-exponential value, but the ratio τ_2/τ_1 is about 1.5. Indeed, the diffusion expected from relation 2 is damped almost immediately, and the exponential term dominates the relaxation. This is consistent with the conclusion reached in the previous section that the number of equivalent kinetic units for C_6 is close to zero. The rather good fit obtained with the GDL model is due more to the loss term than to the specific polymer-like 1-D diffusion term. (Indeed, even the J_0 expression, which corresponds to a single exponential, does not fit too badly the C_6 data.) This probe behaves roughly like a rigid object.

When n is increased, τ_2/τ_1 increases, but the quality-of-fit for the GDL model gets significantly worse than for the 2-exponential expression. (Compare the GDL and 2-exponential best fits, Table II, and Figure 5, parts a and b, for C_8 and C_{10}.) These probes probably correspond to

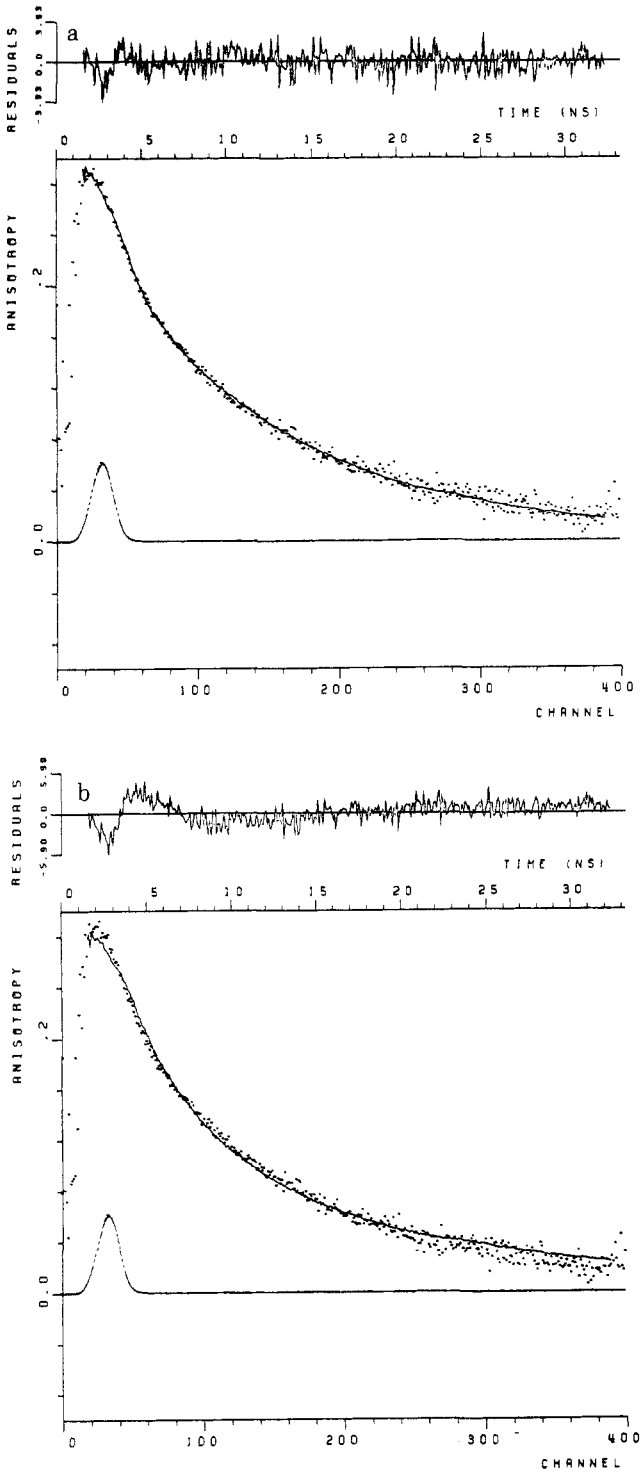

Figure 5. Best-fit 2-exponentials (a) and GDL (b) expressions to the anisotropy of C_{10} at 29.6 °C.

the crossover region in which the internal (polymer-like) and overall motions involve similar time scales. No simple model is expected to describe accurately the dynamics of the probe in this region.

However, for the larger probes of the series, C_{14} and C_{16}, the GDL model reaches values of χ^2 comparable with the 2-exponential ones. (See Table II, and compare Figure 2, parts e and f.) This good fit, which has already been observed in the case of long-chain labeled polybutadiene, indicates that the internal 1-D modes of orientation diffusion dominate the OACF.

From an experimental point of view, it seems important to notice that the GDL model does not fit all the data as well. Through the results obtained with C_8 and C_{10}, the technique shows that it is able to detect without ambiguity a deviation from this model when it has a plausible physical origin. It decreases the risk that the good fits obtained with C_{14}, C_{16}, and labeled polybutadiene[1] were merely a consequence of a good curve-fitting ability of the GDL and HH expressions.

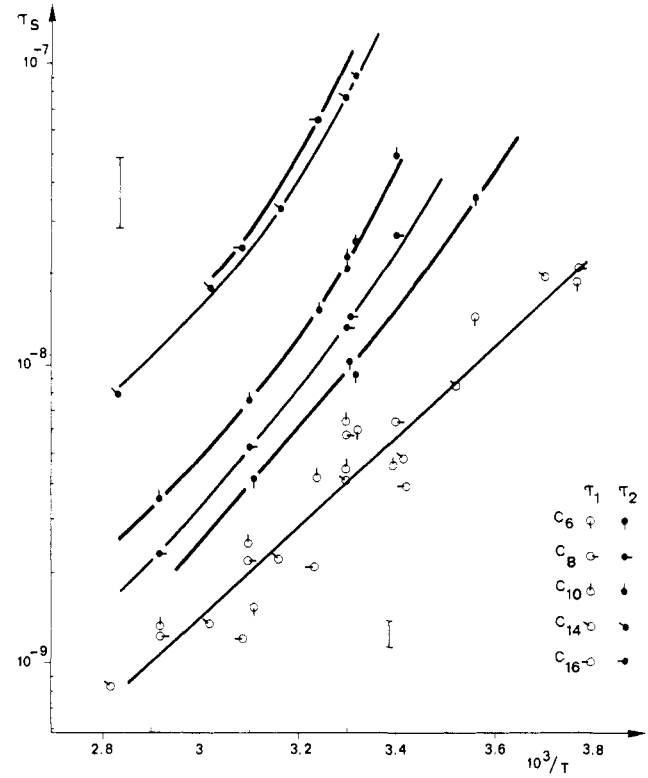

Figure 6. Temperature evolution of the correlation times for the different probes.

The regular increase of the ratio τ_2/τ_1 when n is increased indicates that in the probes investigated here the damping is associated with the length of the mobile tail. However, for C_{14} and C_{16}, the ratio τ_2/τ_1 reaches values similar to the ones obtained previously for labeled polybutadiene. The damping due to chain ends probably decreases in these probes down to a value comparable with the intrinsic damping of the chain or even smaller. This gives the order of magnitude of the scale at which this intrinsic damping occurs, whatever its physical origin is. As discussed previously,[15] the precision on τ_2 in FAD is rather low. In other words, the above scale, i.e., about 16 carbon atoms, is probably close to the distance at which the label ceases being sensitive to remote effects on the chain.

VI. Influence of the Temperature on Correlation Times

Because of its discrete nature, the JS model is not at all convenient to study temperature effects. In the previous section, we have shown that the continuous GDL model accounts very well for the OACF of the largest probes in the series. For the probes C_6 to C_{10}, fitting is imperfect, but it remains generally much better than with the JS expressions. Thus, for lack of more sophisticated theories, we discuss temperature effects by using the GDL model.

The evolution of the correlation times τ_1 and τ_2 as a function of $10^3/T$ is plotted in Figure 6, and the corresponding quantitative results are gathered in Table IV. These results complement the discussion begun in the previous section. For instance, one can observe that at all

Table IV
Correlation Times Obtained by Using the GDL Model for All Probes at all Temperatures

n	$10^3/T$, K^{-1}	τ_1, ns	τ_2, ns	τ_2/τ_1
6	3.77	18.7		
	3.56	14.6	36	2.5
	3.32	6.1	9.2	1.5
	3.11	1.5		
8	3.77	22		
	3.40	6.4	27	4.2
	3.30	5.8	13	2.3
	3.10	2.4	5.3	2.2
	2.92	1.23	2.3	1.8
10	3.54	21.0		
	3.40	4.6	50	11
	3.30	4.4	22	5.1
	3.24	4.2	15	3.5
	3.10	2.5	7.6	3.1
	2.92	1.3	3.5	2.7
14	3.71	19.6		
	3.54	8.2		
	3.42	4.8		
	3.30	4.1	78	19
	3.17	2.2	33	15
	3.04	1.35	18	13
	2.82	0.83	8	9.5
16	3.42	3.9		
	3.24	2.1	67	31
	3.09	1.2	24	19

temperatures the increase in τ_2/τ_1 as a function of n is due entirely to τ_2. At a given temperature, τ_2 increases very continuously for values of n up to 14. In these probes, the damping term associated with τ_2 is due to chain ends. The saturation observed between C_{14} and C_{16} indicates the crossover to the "long chain" situation, in which the damping by chain ends becomes negligible as regards the intrinsic damping (independent of chain length).

The values of τ_2 are rather scattered. This scatter is certainly a consequence of the approximate character of the GDL model for the shortest probes in the series, but it leaves the major difference between τ_1 and τ_2 very apparent.

In contrast with τ_2, τ_1 does not vary with n at the precision of the experiments. In our opinion, this observation is sufficient to confirm rather unambiguously the conformational origin of the 1-D diffusion term with characteristic time τ_1. Of course, the values of τ_1 obtained here must not be identified with the conformational jump time of a pure polyethylene chain. It is the jump time for the particular conformational sequence including the anthracene group, which can differ from the previous one by a factor of 2 or more. Also, one must bear in mind that the motions are strongly coupled with the surrounding polybutadiene chains. The apparent activation energy for τ_1 (about 30 kJ/mol) is not known very precisely because of the scatter, but it is rather close to the one obtained for labeled polybutadiene in the previous study (39 kJ/mol, ref 1). Thus, the conformational motions of the C_n probes are involved in the cooperative activation processes of the surroundings.

Another striking aspect in Table IV and Figure 6 is the variation of τ_2/τ_1 as a function of the temperature for a given probe, which contrasts with the behavior observed for labeled polybutadiene. The behavior observed for the C_n probes implies that the progressive crossover between the "n small" or "dominant damping by the ends" regime and the "n large" or "dominant intrinsic damping" regime depends on the temperature. For instance, if one defines arbitrarily a characteristic value τ_2/τ_1 for this crossover (let's say 10), the length of the alkyl chain necessary to reach this value is about 14 carbon atoms at 355 K, but it is only 10 atoms at 294 K. (See Table IV.) This striking observation is difficult to interpret further because, in the present set of experiments, it can be associated both with changes in conformation distributions, which tend to decrease the overall size of the probes with increasing temperature, and with intermolecular effects related with the free volume.

VII. Conclusions

The series of labeled model molecules synthesized in our laboratory provide an indirect way to explore the dynamic properties of polymer chains simultaneously from temporal and spatial points of view by using fluorescence anisotropy decay. Such a time–space exploration is usually a privilege of neutron quasi-elastic scattering. The present study is more indirect, but it retains all the advantages and performances of modern optical experiments. In particular, the high flux of the synchrotron pulsed light source and the accuracy of the single photon counting technique allow a precise discussion of molecular models.

The major conclusion of the present study is the following: The diffusive nature of the orientation autocorrelation function of a polymer settles on a rather short chain length, about 25–35 carbon atoms in the present study on polyethylene-type probes. This 1-D diffusion certainly corresponds to "cooperative conformation jumps" (in the sense introduced by Helfand[6]), but these jumps are also involved in the overall activation of the surrounding medium. For the largest probes in the series, the orientation autocorrelation function is well described by the generalized diffusion and loss model, but the smallest ones show a more complex behavior, probably because internal and overall motions occur on similar time scales.

Acknowledgment. We are greatly indebted to B. Jasse, C. K. Yeung, and F. Costa-Torro for the synthesis of the probes used in this study and to J. C. Brochon and F. Merola for their support during the experiments at LURE. The technical support of the Michelin Co. is also acknowledged with gratitude.

Registry No. PB (homopolymer), 9003-17-2; 9,10-dihexylanthracene, 98876-31-4; 9,10-dioctylanthracene, 26438-34-6; 9,10-didecylanthracene, 98876-32-5; 9,10-ditetradecylanthracene, 98876-33-6; 9,10-dihexadecylanthracene, 98876-34-7.

References and Notes

(1) Viovy, J. L.; Monnerie, L.; Merola, F. *Macromolecules* **1985**, *18*, 1130.
(2) Williams, G.; Watts, D. C. *Trans. Faraday Soc.* **1971**, *66*, 80.
(3) Valeur, B.; Jarry, J. P.; Geny, F.; Monnerie, L. *J. Polym. Sci., Polym. Phys. Ed.* **1975**, *13*, 667, 675.
(4) Jones, A. A.; Stockmayer, W. H. *J. Polym. Sci., Polym. Phys. Ed.* **1975**, *15*, 847.
(5) Bendler, J. T.; Yaris, R. *Macromolecules* **1978**, *11*, 650.
(6) Hall, C. K.; Helfand, E. *J. Chem. Phys.* **1982**, *77*, 3275.
(7) Viovy, J. L.; Monnerie, L.; Brochon, J. C. *Macromolecules* **1983**, *16*, 1845.
(8) Williams, M. L.; Landel, R. F.; Ferry, J. D. *J. Am. Chem. Soc.* **1955**, *77*, 3701.
(9) Ferry, J. D. "Viscoelastic Properties of Polymers", 2nd ed.; Wiley: New York, 1970.
(10) Yeung, C. K. Thesis, Universite Paris-VI, 1983.
(11) Queslel, J. P. Thesis, Universite Paris-VI, 1982.
(12) Brochon, J. C. In "Protein Dynamics and Energy Transduction"; Ishiwata, S., Ed.; Taniguchi Foundation: Japan, 1980.
(13) Chuang, T. J.; Eisenthal, K. B. *J. Chem. Phys.* **1972**, *57*, 5094.
(14) Viovy, J. L. Doctorat d'Etat, Universite Paris-VI, 1983.
(15) Viovy, J. L.; Monnerie, L. *Adv. Polym. Sci.* **1985**, *67*, 99.
(16) Lassegues, J. C.; Fouassier, M.; Viovy, J. L. *Mol. Phys.* **1983**, *11*, 1.